Cerebral Cortex, July 2021;31: 3177–3183

doi: 10.1093/cercor/bhaa409
Advance Access Publication Date: 17 February 2021
Original Article

ORIGINAL ARTICLE

Paucity of Entorhinal Cortex Pathology of the Alzheimer's Type in SuperAgers with Superior Memory Performance

Tamar Gefen[1,2], Allegra Kawles[1], Beth Makowski-Woidan[1], Janessa Engelmeyer[1], Ivan Ayala[1], Payam Abbassian[1], Hui Zhang[1,3], Sandra Weintraub[1,2], Margaret E. Flanagan[1,4], Qinwen Mao[1,4], Eileen H. Bigio[1,4], Emily Rogalski[1,2], M. Marsel Mesulam[1,5] and Changiz Geula[1,6]

[1]Mesulam Center for Cognitive Neurology and Alzheimer's Disease, Northwestern University Feinberg School of Medicine, Chicago, IL 60611, USA, [2]Department of Psychiatry and Behavioral Sciences, Northwestern University Feinberg School of Medicine, Chicago, IL 60611, USA, [3]Department of Preventive Medicine, Northwestern University Feinberg School of Medicine, Chicago, IL 60611, USA, [4]Department of Pathology, Northwestern University Feinberg School of Medicine, Chicago, IL 60611, USA, [5]Department of Neurology, Northwestern University Feinberg School of Medicine, Chicago, IL 60611, USA and [6]Department of Cell and Developmental Biology, Northwestern University Feinberg School of Medicine, Chicago, IL 60611, USA

Address correspondence to Tamar Gefen, Mesulam Center for Cognitive Neurology and Alzheimer's Disease, Northwestern University, 300 E. Superior Street, Tarry Building, 8th Floor, Chicago, IL 60611, USA. Email: tamar.gefen@northwestern.edu.

Abstract

Advancing age is typically associated with declining memory capacity and increased risk of Alzheimer's disease (AD). Markers of AD such as amyloid plaques (AP) and neurofibrillary tangles (NFTs) are commonly found in the brains of cognitively average elderly but in more limited distribution than in those at the mild cognitive impairment and dementia stages of AD. Cognitive SuperAgers are individuals over age 80 who show superior memory capacity, at a level consistent with individuals 20–30 years their junior. Using a stereological approach, the current study quantitated the presence of AD markers in the memory-associated entorhinal cortex (ERC) of seven SuperAgers compared with six age-matched cognitively average normal control individuals. Amyloid plaques and NFTs were visualized using Thioflavin-S histofluorescence, 6E10, and PHF-1 immunohistochemistry. Unbiased stereological analysis revealed significantly more NFTs in ERC in cognitively average normal controls compared with SuperAgers ($P < 0.05$) by a difference of ~3-fold. There were no significant differences in plaque density. To highlight relative magnitude, cases with typical amnestic dementia of AD showed nearly 100 times more entorhinal NFTs than SuperAgers. The results suggest that resistance to age-related neurofibrillary degeneration in the ERC may be one factor contributing to preserved memory in SuperAgers.

Key words: Alzheimer's disease, entorhinal cortex, memory, stereology, SuperAgers

Introduction

It is well known that age is the most prominent risk factor for the development of Alzheimer's disease (AD), characterized by pathologic hallmarks including neurofibrillary tangles (NFTs) and amyloid plaques (APs). These hallmarks accumulate with age in the cognitively average or "normal" human brain in lower density and restricted distribution, likely giving rise to memory complaints in the elderly. Age-related memory decline is so common that normative values developed for neuropsychological assessment incorporate age-related adjustments. The Northwestern University SuperAging project has shown that it is possible to maintain youthful memory performance beyond the eighth decade. SuperAgers (SAs) are defined by chronologic age and neuropsychologic performance; they are 80+-year-olds with episodic memory performance that is at least as good as what would be considered normal for 50- to 60-year-olds. These unique individuals are committed to longitudinal assessment and brain donation. The presence of a cohort with such superior performance offers unique opportunities for exploring mechanisms underlying concepts of "resistance," "resilience," and "cognitive reserve" (Stern et al. 2019).

Our prior studies have identified biologic, psychosocial, and genetic features of the SAs (Harrison et al. 2012; Rogalski et al. 2013, 2018; Gefen et al. 2014, 2015, 2018; Cook et al. 2017; Cook Maher et al. 2017; Huentelman et al. 2018; Janeczek et al. 2018). We have shown that compared with their age-matched cognitively average-for-age peers, SAs show decreased rate of cortical thinning (Harrison et al. 2012; Rogalski et al. 2013; Cook et al. 2017), greater volume of anterior cingulate cortex (ACC), greater density of Von Economo neurons (Rogalski et al. 2013; Gefen et al. 2018), lower acetylcholinesterase activity in cortical pyramidal neurons (Janeczek et al. 2018), lower densities of microglia in white matter (Gefen et al. 2019), and distinct polymorphisms of the MAP2K3 gene (Huentelman et al. 2018). Given these distinguishing factors, one lingering question is whether SAs are immune to the development of age-related involutional influences. If so, is the immunity based on resistance to the emergence of age-related structural changes in the brain (e.g., the plaques and tangles of AD) or on a resilience of brain function to pathologic changes?

The current study quantitatively evaluated the presence of AD pathology in the memory-associated entorhinal cortex (ERC) in postmortem samples from SAs compared with age-matched cognitively average elderly individuals (normal controls [NCs]) (Rogalski et al. 2013). Our prior reports have documented relatively low NFT burden according to the Braak staging schema in limbic and cortical regions (Rogalski et al. 2019). Here, we employ a comprehensive stereological approach that allows for a finer-grained analysis in these two groups, with detailed quantitation for robust estimates of APs and tau NFTs in the ERC. Findings help address questions related to "resistance" to the emergence of degenerative pathology in limbic regions or "resilience" to their influence on cognitive function. The integration of these findings with prior and future studies of this SuperAging cohort will elucidate the biologic drivers of superior memory performance in aging.

Materials and Methods

Case Selection and Inclusion Criteria

Brain autopsies were identified from cases held within the Northwestern University Alzheimer's Disease Center Brain Bank, based on criteria required to obtain status as either "SuperAger" or as an age-matched cognitively average NC participant, described below. Seven right-handed Cognitive SAs and 6 right-handed cognitively average (normal) controls met criteria for inclusion in this study. All participants were required to lack clinical evidence or history of neurologic disease. Written informed consent and agreement to enter the brain donation program were obtained from all participants in the study, and the study was approved by the Northwestern University Institutional Review Board and in accordance with the Helsinki Declaration (www.wma.net/en/30publications/10policies/b3/). All participants were required to have preserved activities of daily living.

SuperAging participants are required to meet psychometric criteria on a battery of neuropsychological tests, which were chosen for their relevance to cognitive aging and their sensitivity to detect clinical symptoms associated with dementia of the Alzheimer's type (Weintraub et al. 2012). These criteria have been described in detail in prior reports (Rogalski et al. 2013, 2019; Gefen et al. 2014, 2015). Five of 7 SAs included in this analysis met criteria within 1 year prior to death; two additional cases that fulfilled the SA criteria were identified through retrospective chart review. SuperAging criteria is based in part on the delayed recall score (30 min) of the Rey Auditory Verbal Learning Test (RAVLT) (Schmidt 2004), which is used as a measure of episodic memory with performance in SAs required to be at or above average normative values for individuals in their 50s and 60s (midpoint age = 61 years; RAVLT delayed recall raw score $\geq$ 9; RAVLT delayed recall scaled score $\geq$ 10). A 30-item version of the Boston Naming Test (BNT-30; Saxton et al. 2000), Trail-Making Test Part B (TMT Part B; Reitan 1958), and Category Fluency test ("Animals" Morris et al. 1989) were used to measure cognitive function in nonmemory domains. On the BNT-30, TMT Part B, and Category Fluency, SAs were required to perform within or above 1 standard deviation (SD) of the average range for their age and demographics according to published psychometric norms (Ivnik et al. 1996; Heaton et al. 2004; Shirk et al. 2011). In general, the cognitively average NCs are age-matched and are required to score within 1 SD of the average range for their age and education according to published psychometric norms on the same neuropsychological measures administered to the SAs. If comprehensive neuropsychological testing was unavailable for cognitively average NCs, the holdings of the brain bank were surveyed to identify cases that were cognitively normal based on age and without evidence of cognitive impairment or complaints. See Gefen et al. (2015) and Gefen et al. (2018) for more information on these criteria. See Table 1 for demographic and participant information.

Tissue Processing and Histopathologic Evaluation

Each brain was cut into 3- to 4-cm coronal blocks and fixed in 4% paraformaldehyde for 30–36 h at 4 °C and then taken through sucrose gradients (10–40% in 0.1 M sodium phosphate buffer, pH 7.4) for cryoprotection and stored at 4 °C. Blocks were sectioned at a thickness of 40 µm on a freezing microtome and stored in 0.1 M phosphate buffer containing 0.02% sodium azide at 4 °C until use. Postmortem intervals ranged from 4 to 58 h. Samples from representative brain regions of each case were surveyed qualitatively by a neuropathologist (E.H.B.). The region investigated was equivalent across tissue blocks and taken from the anterior portion of the ERC, corresponding to the rostral

Table 1 Case information and demographics

Case	Age at death (years)	Sex	Education (years)	Testing obtained ante-mortem (months)	MMSE (/30)	Premorbid intelli-gence	PMI[a]	ApoE	CERAD	Brain weight	Braak staging	Non-Alzheimer pathology
SA 1	87	F	12	1	29	133[b]	NA	∈3/∈3	2	1240	III	ARTAG, AGD
SA 2	90	F	18	1	29	135[b]	4	∈3/∈3	0	990	II–III	1 remote lacunar infarct, left globus pallidus
SA 3	99	F	16	4	25	112[b]	58	∈3/∈3	3	1020	III	Multiple cortical microinfarcts (nonsignificant); 1 remote lacunar infarct, left putamen; ARTAG, AGD
SA 4	87	F	18	5	30	119[b]	11	∈3/∈3	3	1090	II–III	ARTAG
SA 5	81	F	18	8	30	106.76[c]	9.5	∈3/∈3	1	1269	0-I	None
SA 6	90	F	14	8	29	110.81[c]	5	∈2/∈3	0	1100	II–III	PART (definite), Lewy body in dorsal motor nucleus of vagus (incidental), ARTAG
SA 7	95	F	18	12	NA	113.81[c]	5	NA	0	1241	0	None
NC 1	77	F	NA	NA	NA	NA	42	NA	1	1200	III	NA
NC 2	89	F	16	21	29	138[b]	6	∈2/∈3	2	1160	III–IV	Vascular disease
NC 3	96	F	14	14	NA	NA	5	NA	0	NA	IV	Mild ischemic changes
NC 4	88	M	12	11	28	100.81[c]	12	NA	1	1250	III–IV	Infarct, right temporal lobe
NC 5	82	M	NA	NA	NA	NA	24	NA	0	NA	III	NA
NC 6	95	F	12	4	28	108.34[c]	3.25	∈2/∈3	2	1096	III	None

Note: Cognitive measures were not identical for all participants and cognitive scores are provided as actual/total possible score. PMI, postmortem interval.
[a]ARTAG, aging-related tau astrogliopathy; AGD, argyrophilic grain disease; PART, primary age-related tauopathy; NA, not available. Note, in cases noted as "None," TDP-43 staining was not available.
[b]WAIS-III FSIQ.
[c]Barona Index premorbid intelligence estimate ($M = 100$; SD 15) (Barona et al. 1984); Braak staging followed published guidelines (Braak and Braak 1991, 1993); neuritic plaque score (0, 1, 2, or 3) was determined by the method of the Consortium to Establish a Registry for Alzheimer's Disease (CERAD) (Mirra et al. 1991).

sector of Brodmann area 28. Within each block, the start of the section sampling was randomized per the requirement of stereologic counting principles. Up to 6 sections (intersection interval = 24 or 54) in each cortical region were stained with 0.1% Thioflavin-S (Sigma Aldrich), which recognizes β-pleated sheet protein conformations, to visualize NFTs and mature/-compact APs.

In a small subset of cases (SA 4, 6, and 7; and NC 2, 3, and 4), the mouse monoclonal antibody PHF-1 (generous gift of the late Dr Peter Davies, Albert Einstein College of Medicine, NY, 1/1000) was used employing the Vectastain Elite ABC Kit (Vector Laboratories). PHF-1 recognizes tau phosphorylated at Ser396/404 and allows for additional visualization of tangles and pre-tangles in ERC (see Fig. 1C,D). The 6E10 antibody (monoclonal mouse anti-Aβ 1–16) was used to visualize all plaques, mature and diffuse, via Aβ immunohistochemical processing in this smaller cohort of select SAs and cognitively average NCs. Braak staging according to published guidelines (Braak and Braak 1991; Braak et al. 1993) was also determined in each case to identify NFT involvement in transentorhinal/ERC, other limbic cortical areas, and neocortical regions. The Consortium to Establish a Registry for AD (CERAD) protocol was used to determine neuritic plaque scoring (Mirra et al. 1991; Montine et al. 2012).

SuperAging cases were evaluated for the presence of secondary pathologies (Table 1). Four SAs showed age-related tau astrogliopathy, a pathological entity that encompasses a number of glial abnormalities frequently observed in the brains of elderly (Kovacs et al. 2016); 2 evidenced argyrophilic grain disease; 2 showed at least one infarct, and 1 SA showed primary age-related tauopathy (Crary et al. 2014). Secondary pathologies on cognitively average NC cases were not available, with the exception of one, which showed evidence of vascular disease. Apolipoprotein (ApoE) genotyping was available for 8 out of 13 cases (6 SAs and 2 cognitively average NCs), with none showing the presence of an ApoE∈4 allele.

Quantitation of AP and NFT Pathology in ERC

Modified stereological methods were used to estimate the density of Thioflavin-S-stained plaques and tangles as previously reported (Gefen et al. 2012), using fluorescent (380–420 nm) microscopy on whole hemisphere frozen sections. In a subset of cases (3 SAs and 3 cognitively average NCs; SA 4, 6, and 7 and NC 2, 3, and 4), we performed modified unbiased stereology in ERC stained immunohistochemically with PHF-1 to visualize pre-NFTs and mature NFTs. Briefly, per case, the ERC region was traced at 4× and analyzed at 40× magnification by an individual "blinded" to group. Analysis was performed on up to 6 sections according to procedures previously described in detail (Geula et al. 2003) using the fractionator method and the

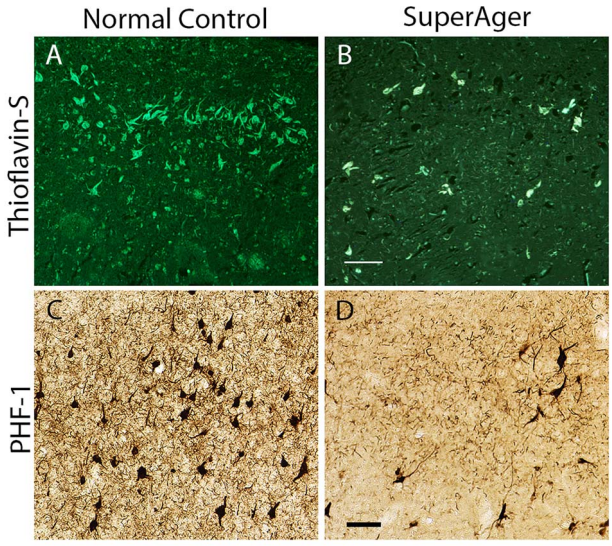

Figure 1. (*A–D*) NFTs in the ERC of a SA and age-matched cognitively average NC visualized with Thioflavin-S and PHF-1. (*A,B*) Thioflavin-S staining from paraffin-embedded tissue in the ERC at 10× in NC2 and SA2. (*C,D*) PHF-1 staining from frozen sections of ERC at 10× in NC2 and SA 2 shows comparable tangle pathology. Scale bars indicate 100 µm.

StereoInvestigator software from MicroBrightField Biosciences. The sections used in analysis were treated as adjacent sections, allowing for calculation of the density in the total volume within the sections. Each region to be studied was traced from the cortical surface to the white matter. The top and bottom 2 µm of each section were set as guard height. The dimensions of the counting frame chosen were 170 × 170 µm based on trials. For each set of stereologic markers, the coefficient of error was calculated and sampling parameters were adjusted so that the coefficient of error was < 0.1. Data were expressed as counts per cubic millimeter based on planimetric calculation of volume by the fractionator software. Counts included NFTs and/or APs, and mean regional densities were compared among the two groups.

In a subsequent analysis, we quantified Aβ immunohistochemistry using the 6E10 antibody in addition to Thioflavin-S, to report all plaques including those that are mature and diffuse. The area fraction fractionator method (StereoInvestigator software) was performed to provide an unbiased estimate of plaque load in the ERC, with 3 sections chosen randomly per case. Based on trials, the counting grid was set to 1217.59 × 600.85 µm. An estimate of the area fraction occupied by plaques was calculated per group.

Statistical Analysis

Data were analyzed using nonparametric Mann–Whitney rank-sum *t*-tests for between-group (SA vs. NCs) differences in Thio-S-positive entorhinal pathology. Dependent variables were estimate densities of NFTs and APs. A $P < 0.05$ was considered significant. Statistical analysis was performed using GraphPad Prism version 8.

Results

There were no significant differences in postmortem interval, years of education, or age at death between NCs and SAs. The entire sample was predominantly female (11 of 13) and so evaluation of sex differences was not possible.

On average, NCs showed significantly more Thio-S-positive NFTs in ERC compared with SAs ($P = 0.0367$), by an order of approximately 3-fold (SA mean NFT = ~210 per mm^3 vs. NC mean NFT = ~650 per mm^3) (Fig. 2A,B). No statistically significant differences were detected in Thio-S-positive plaque density between cognitively average NCs and SAs (SA mean AP = ~9 per mm^3 vs. NC mean AP = ~15 per mm^3). There was also no difference observed in Aβ (6E10) plaque load in the ERC region between SAs and cognitively average NCs. Both the SA and cognitively average NC cases showed an average area fraction of plaques of ~0.015 (SD = 0.012 and 0.015, respectively).

At the individual level, 8 of the total 13 cases (5 SAs and 3 NCs) showed no Thio-S-positive APs in ERC using stereological analysis, reflecting either no or extremely sparse density. The other 5 cases showed very low AP counts that ranged from ~8 to 39 counts of APs per mm^3, also very sparse. There was overlap and variability in AP (Fig. 2B) and NFT (Fig. 2A) counts where one SA case (SA 7) showed no tangles based on stereological quantitation in ERC; when viewed qualitatively at 4× and 20×, there were approximately 1–2 Thio-S-positive NFTs visualized in ERC. In this case, no plaques were encountered in ERC based on stereological quantitation. All other SuperAging cases ($N = 6$) and all NCs showed at least sparse Thio-S-positive NFTs in ERC.

We performed modified unbiased stereology in ERC stained immunohistochemically with PHF-1 to visualize pre-NFTs and mature NFTs in a subset of 3 SAs (SA 4, 6, and 7) and 3 NCs (NC 2, 3, and 4). PHF-1-positive NFTs in SAs were estimated to be 163.9 per mm^3 versus an estimated 2333.5 per mm^3 in the NC group. These counts are consistent with Thio-S-positive NFT patterns (Fig. 1), and as expected, they showed overall "higher" numbers than Thio-S-positive densities accounting for both pre-NFTs and mature NFTs.

In general, the Braak staging of NFTs in SAs ranged from 0 to III, whereas the range in normal elderly fell between III and IV; and as expected, only SAs showed Braak stages of 0–I. To highlight the utility of a careful stereologic quantitation to distinguish these two groups, Mann–Whitney rank-sum *t*-tests were performed comparing NFTs in SAs versus NCs, but excluding the two SAs with Braak stages of 0–1. Although this exploratory analysis did not reach significance ($P = 0.1234$), the mean raw counts demonstrated that SA cases (mean = ~290) had less than half the number of ERC tangles compared with the NC group (mean = ~650 per mm^3). The Braak staging scheme, while invaluable to pathologic evaluation, is nonetheless a coarse estimate of Thio-S-positive NFT burden, and our stereologic findings are able to demonstrate with granularity quantitative differences between SAs and NCs in ERC.

To place these data within the context of AD, we returned to data obtained from a stereologic study that quantitated Thio-S-positive plaques and tangles in 5 participants with dementia of the Alzheimer type (DAT) and pathologic AD at postmortem examination (Gefen et al. 2012). Age at death of the 5 DAT cases ranged from 71 to 89 (2 males, 3 females), and all cases showed either Braak staging V or VI. In this study, three adjacent sections from paraffin-embedded ERC of participants were stained with 1.0% Thioflavin-S (Sigma-Aldrich). With the exception of a difference in section thickness (cut at 5 µm) given paraffin embedding and counting parameters at 60×, other stereologic parameters were nearly identical and therefore estimates are expected to be comparable. Mean NFTs were estimated to be 20 956 per mm^3 (average of left and right ERC), and mean APs

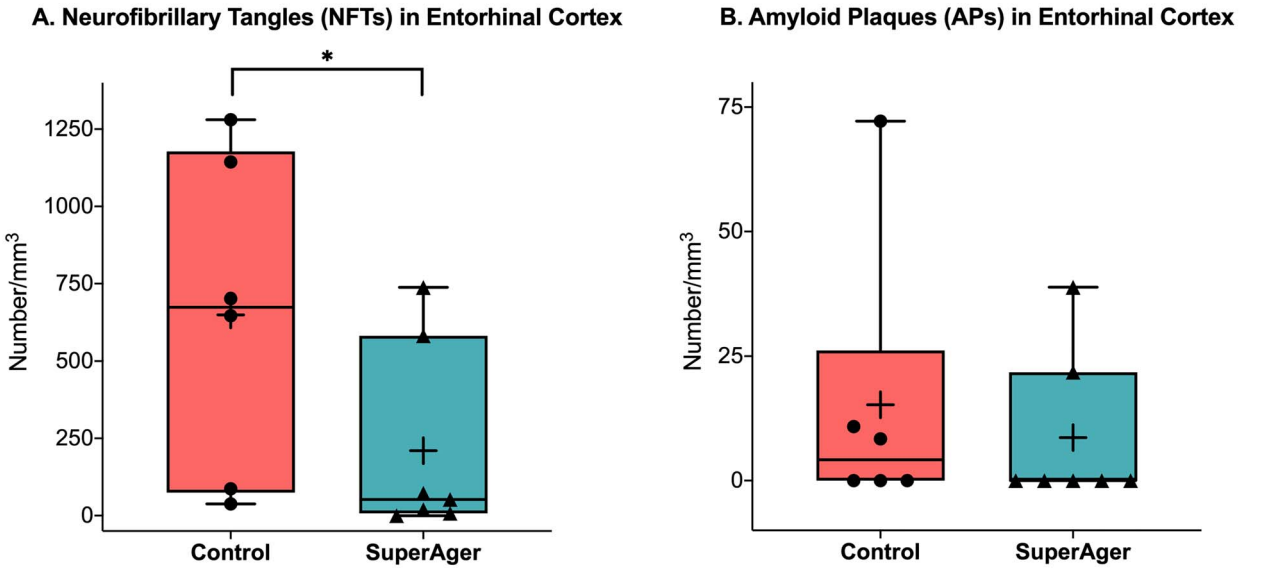

Figure 2. Stereological density (number/mm^3) of Thioflavin-S-positive NFTs (*A*) and APs (*B*) in the ERC of SAs versus age-matched cognitively average NCs. The middle, upper, and lower horizontal lines in the box plot represent the median, 75th, and 25th percentiles, respectively. The end of the vertical extensions above and below the box represents the extreme value that is at most 1.5 times the interquartile range above the 75th percentile or below the 25th percentile. The "+" represents the mean. *$P < 0.05$.

were estimated to be 937 per mm^3. The number of ERC NFTs in the previously reported DAT group is remarkable when contrasted with ~210 per mm^3 NFTs in the ERC of SAs, a nearly 100-fold difference.

Discussion

One of the major goals of the Northwestern University SuperAging project is to explore the neurobiologic mechanisms of resilience and resistance to brain aging and Alzheimer's disease. These are dynamic terms, in flux at present, representing multiple constructs unique to cognitive aging. Our SuperAging study was designed to ask whether there are protective factors that counter age-related involutional processes by promoting resistance to the emergence of degenerative features in the brain or resilience to their influence on cognitive function. Our established and dedicated cohort of "SuperAgers" appears to resist memory decline expected in average (normal) aging. These participants undergo longitudinal assessment and brain donation.

One prior stereologic study of this cohort observed that SAs showed less AD pathology in cingulate cortex (Gefen et al. 2015) and another introduced Braak staging in SAs compared with NCs (Rogalski et al. 2013). In the latter study, SAs as a group tended to affiliate with lower Braak stages, though with some exceptions. The current study addressed the question of limbic predominant Alzheimer pathology through an in-depth stereologic study that quantitated the presence of Thio-S-positive APs and NFTs in ERC in groups of SAs and cognitively normal individuals, who showed no differences at the group level in age at death. There are 3 main conclusions. The first is that the density of NFTs in the ERC in cognitively normal elderly individuals was significantly higher than those in SAs, by a difference of about 3-fold. We reference our prior stereologic quantitation using similar methodology in which cases with typical amnestic dementia of AD had nearly 100 times more entorhinal NFTs than SAs (Gefen et al. 2012). Second, there were no significant differences in plaque density between the two groups, a finding that was not surprising given weak relationships found between plaque burden and cognitive status (Guillozet et al. 2003). Finally, we highlight that the Braak staging system, though invaluable to pathologic assessment, is nonetheless coarse; indeed, studies that employ unbiased quantitative analyses of limbic regions can add archival and meaningful information that allow for granular comparisons of pathology (Furcila et al. 2019).

Our findings indicate that the majority of SAs remain at Braak stages of NFT formation that are unusually low based on age, suggesting that they are resistant to the emergence of NFTs, while other SAs seem resilient to the effects of neurofibrillary degeneration on cognition, having superior memory performance even at Braak stages that overlap with those seen in cognitively normal elderly controls (Rogalski et al. 2013). In a qualitative survey of our first 10 SA brains (Rogalski et al. 2019), the hippocampus and ERC contained healthy appearing neurons with neurofibrillary degeneration even in those cases that were in the Braak II–III stages. To unravel the neural basis of either of these associations, our future studies will examine other putative factors relating to cellular degeneration including neuronal integrity, dendritic extent, status of white matter, and integrity of synapses. The question of comorbid pathology in the aging brain is also relevant and timely. The new limbic predominant age-related transactive response DNA-binding protein 43 (TDP-43) encephalopathy neuropathological change (LATE-NC) classification (Nelson et al. 2019) was developed recently to describe inclusions containing hyperphosphorylated TDP-43 that appear in limbic structures in individuals over age 65 with an amnestic syndrome. The relationship between TDP-43, hippocampal integrity, and cognitive performance is still nebulous, with one study showing that in cases with comorbid AD and TDP-43,

TDP-43 is associated independently with cognitive impairment (Nelson et al. 2010). In the current study, when available, SAs and NCs did not tend to show comorbid TDP-43. Limitations of this study include minimal attention to TDP-43, the small sample size, lack of neuronal counts to account for overall density in ERC, and overrepresentation of females in our sample. To date, it is unclear whether there are biological sex differences that affect SuperAging status. In general, future investigations will be dedicated to addressing these questions in larger samples from this cohort.

Some individuals who have been described as aging "successfully" show normative episodic memory decline, which is consistently correlated with altered hippocampal volume/function and reduced functional connectivity among other cortical networks (e.g., default mode) (Sun et al. 2016). Our initial cross-sectional studies established the remarkable fact that SAs have larger cortical volumes than their same-aged elderly controls and no significant thinning relative to cognitively average middle-aged adults in their 50s and 60s (Harrison et al. 2012). The ACC of the paralimbic network was even thicker in the SAs than middle-aged controls and showed very little AD pathology (Gefen et al. 2015). Comparative studies in humans and other higher-order mammalian species show abundant axonal and synaptic interconnectivity that is bidirectional from limbic and paralimbic areas to cortex. Observations from studies of neurodegenerative diseases like typical AD where neuronal loss appears to spread preferentially from limbic to cortical networks (Mesulam 2012) are crucial to understanding both cognitive function and dysfunction. Exploring these circuits in autopsied human brain samples from SAs will offer more exciting insights into resistance versus resilience, selective vulnerability of anatomic regions to disease, and principles of human connectivity in the aged.

Funding

Research reported in this manuscript was supported by the National Institute on Aging of the National Institute of Health under award numbers (P30AG013854, R01AG045571, 1R01AG067781, R01AG062566, R56AG045571).

Notes

We sincerely thank the research participants of the Northwestern SuperAging Research Program and the Northwestern University Alzheimer's Disease Center for their invaluable contributions to this study and the brain donation program. *Conflict of Interest*: None declared.

References

Braak H, Braak E. 1991. Neuropathological stageing of Alzheimer-related changes. *Acta Neuropathol*. 82:239–259.

Braak H, Braak E, Bohl J. 1993. Staging of Alzheimer-related cortical destruction. *Eur Neurol*. 33:403–408.

Cook AH, Sridhar J, Ohm D, Rademaker A, Mesulam MM, Weintraub S, Rogalski E. 2017. Rates of cortical atrophy in adults 80 years and older with superior vs average episodic memory. *JAMA*. 317(13):1373–1375.

Cook Maher A, Kielb S, Loyer E, Connelley M, Rademaker A, Mesulam MM, Weintraub S, McAdams D, Logan R, Rogalski E. 2017. Psychological well-being in elderly adults with extraordinary episodic memory. *PLoS One*. 12(10):e0186413.

Crary JF, Trojanowski JQ, Schneider JA, Abisambra JF, Abner EL, Alafuzoff I, Arnold SE, Attems J, Beach TG, Bigio EH, et al. 2014. Primary age-related tauopathy (PART): a common pathology associated with human aging. *Acta Neuropathol*. 128(6):755–766.

Furcila D, Dominguez-Alvaro M, DeFelipe J, Alonso-Nanclares L. 2019. Subregional density of neurons, neurofibrillary tangles and amyloid plaques in the hippocampus of patients with Alzheimer's disease. *Front Neuroanat*. 13:99.

Gefen T, Gasho K, Rademaker A, Lalehzari M, Weintraub S, Rogalski E, Wieneke C, Bigio E, Geula C, Mesulam M-M. 2012. Clinically concordant variations of Alzheimer pathology in aphasic versus amnestic dementia. *Brain*. 135(5):1554–1565.

Gefen T, Kim G, Bolbolan K, Geoly A, Ohm D, Oboudiyat C, Shahidehpour R, Rademaker A, Weintraub S, Bigio EH, et al. 2019. Activated microglia in cortical white matter across cognitive aging trajectories. *Frontiers in Aging Neuroscience*. 11:94.

Gefen T, Papastefan ST, Rezvanian A, Bigio EH, Weintraub S, Rogalski E, Mesulam MM, Geula C. 2018. Von Economo neurons of the anterior cingulate across the lifespan and in Alzheimer's disease. *Cortex*. 99:69–77.

Gefen T, Peterson M, Papastefan ST, Martersteck A, Whitney K, Rademaker A, Bigio EH, Weintraub S, Rogalski E, Mesulam MM, et al. 2015. Morphometric and histologic substrates of cingulate integrity in elders with exceptional memory capacity. *J Neurosci*. 35(4):1781–1791.

Gefen T, Shaw E, Whitney K, Martersteck A, Stratton J, Rademaker A, Weintraub S, Mesulam MM, Rogalski E. 2014b. Longitudinal neuropsychological performance of cognitive SuperAgers. *J Am Geriatr Soc*. 62(8):1598–1600.

Geula C, Bu J, Nagykery N, Scinto LF, Chan J, Joseph J, Parker R, Wu CK. 2003. Loss of calbindin-D28k from aging human cholinergic basal forebrain: relation to neuronal loss. *J Comp Neurol*. 455(2):249–259.

Guillozet AL, Weintraub S, Mash DC, Mesulam MM. 2003. Neurofibrillary tangles, amyloid, and memory in aging and mild cognitive impairment. *Arch Neurol*. 60(5):729–736.

Harrison TM, Weintraub S, Mesulam MM, Rogalski E. 2012. Superior memory and higher cortical volumes in unusually successful cognitive aging. *J Int Neuropsychol Soc*. 18(6):1081–1085.

Heaton R, Miller S, Taylor M, Grant I. 2004. *Revised comprehensive norms for an expanded Halstead-Reitan battery: demographically adjusted neuropsychological norms for African American and Caucasian adults*. Lutz (FL): Psychological Assessment Resources, Inc.

Huentelman MJ, Piras IS, Siniard AL, De Both MD, Richholt RF, Balak CD, Jamshidi P, Bigio EH, Weintraub S, Loyer ET, et al. 2018. Associations of MAP2K3 gene variants with superior memory in SuperAgers. *Front Aging Neurosci*. 10(155).

Ivnik RJ, Malec JF, Smith GE, Tangalos EG, Petersen RC. 1996. Neuropsychological tests' norms above age 55: COWAT, BNT, MAE token, WRAT-R reading, AMNART, STROOP, TMT, and JLO. *Clin Neuropsychol*. 10(3):262–278.

Janeczek M, Gefen T, Samimi M, Kim G, Weintraub S, Bigio E, Rogalski E, Mesulam MM, Geula C. 2018. Variations in acetylcholinesterase activity within human cortical pyramidal neurons across age and cognitive trajectories. *Cereb Cortex*. 28(4):1329–1337.

Kovacs GG, Ferrer I, Grinberg LT, Alafuzoff I, Attems J, Budka H, Cairns NJ, Crary JF, Duyckaerts C, Ghetti B, et al. 2016.

Aging-related tau astrogliopathy (ARTAG): harmonized evaluation strategy. *Acta Neuropathol*. 131(1):87–102.

Mesulam M. 2012. The evolving landscape of human cortical connectivity: facts and inferences. *Neuroimage*. 62(4):2182–2189.

Mirra SS, Heyman A, McKeel D, Sumi SM, Crain BJ, Brownlee LM, Vogel FS, Hughes JP, van Belle G, Berg L. 1991. The Consortium to Establish a Registry for Alzheimer's disease (CERAD). Part II. Standardization of the neuropathologic assessment of Alzheimer's disease. *Neurology*. 41(4):479–486.

Montine TJ, Phelps CH, Beach TG, Bigio EH, Cairns NJ, Dickson DW, Duyckaerts C, Frosch MP, Masliah E, Mirra SS, et al. 2012. National Institute on Aging-Alzheimer's Association guidelines for the neuropathologic assessment of Alzheimer's disease: a practical approach. *Acta Neuropathol*. 123(1):1–11.

Morris JC, Heyman A, Mohs RC, Hughes JP, van Belle G, Fillenbaum G, Mellits ED, Clark C. 1989. The Consortium to Establish a Registry for Alzheimer's disease (CERAD). Part I. Clinical and neuropsychological assessment of Alzheimer's disease. *Neurology*. 39(9):1159–1165.

Nelson PT, Abner EL, Schmitt FA, Kryscio RJ, Jicha GA, Smith CD, Davis DG, Poduska JW, Patel E, Mendiondo MS, et al. 2010. Modeling the association between 43 different clinical and pathological variables and the severity of cognitive impairment in a large autopsy cohort of elderly persons. *Brain Pathol*. 20(1):66–79.

Nelson PT, Dickson DW, Trojanowski JQ, Jack CR, Boyle PA, Arfanakis K, Rademakers R, Alafuzoff I, Attems J, Brayne C, et al. 2019. Limbic-predominant age-related TDP-43 encephalopathy (LATE): consensus working group report. *Brain*. 142(6):1503–1527.

Reitan RM. 1958. Validity of the trail making test as an indicator of organic brain damage. *Percept Motor Skills*. 8:271–276.

Rogalski E, Gefen T, Mao Q, Connelly M, Weintraub S, Geula C, Bigio EH, Mesulam MM. 2018. Cognitive trajectories and spectrum of neuropathology in SuperAgers: the first 10 cases. *Hippocampus*. 29(5):458–467.

Rogalski E, Gefen T, Mao Q, Connelly M, Weintraub S, Geula C, Bigio EH, Mesulam MM. 2019. Cognitive trajectories and spectrum of neuropathology in SuperAgers: the first 10 cases. *Hippocampus*. 29(5):458–467.

Rogalski EJ, Gefen T, Shi J, Samimi M, Bigio E, Weintraub S, Geula C, Mesulam MM. 2013. Youthful memory capacity in old brains: anatomic and genetic clues from the Northwestern SuperAging project. *J Cogn Neurosci*. 25(1):29–36.

Saxton J, Ratcliff G, Munro CA, Coffey EC, Becker JT, Fried L, Kuller L. 2000. Normative data on the Boston Naming Test and two equivalent 30-item short forms. *Clin Neuropsychol*. 14(4):526–534.

Schmidt M. 2004. *Rey Auditory Verbal Learning Test: a handbook*. Los Angeles: Los Angeles Western Psychological Services.

Shirk SD, Mitchell MB, Shaughnessy LW, Sherman JC, Locascio JJ, Weintraub S, Atri A. 2011. A web-based normative calculator for the uniform data set (UDS) neuropsychological test battery. *Alzheimers Res Ther*. 3(6):32.

Stern Y, Barnes CA, Grady C, Jones RN, Raz N. 2019. Brain reserve, cognitive reserve, compensation, and maintenance: operationalization, validity, and mechanisms of cognitive resilience. *Neurobiol Aging*. 83:124–129.

Sun FW, Stepanovic MR, Andreano J, Barrett LF, Touroutoglou A, Dickerson BC. 2016. Youthful brains in older adults: preserved neuroanatomy in the default mode and salience networks contributes to youthful memory in Superaging. *J Neurosci*. 36(37):9659–9668.

Weintraub S, Wicklund AH, Salmon DP. 2012. The neuropsychological profile of Alzheimer disease. *Cold Spring Harb Perspect Med*. 2(4):a006171.